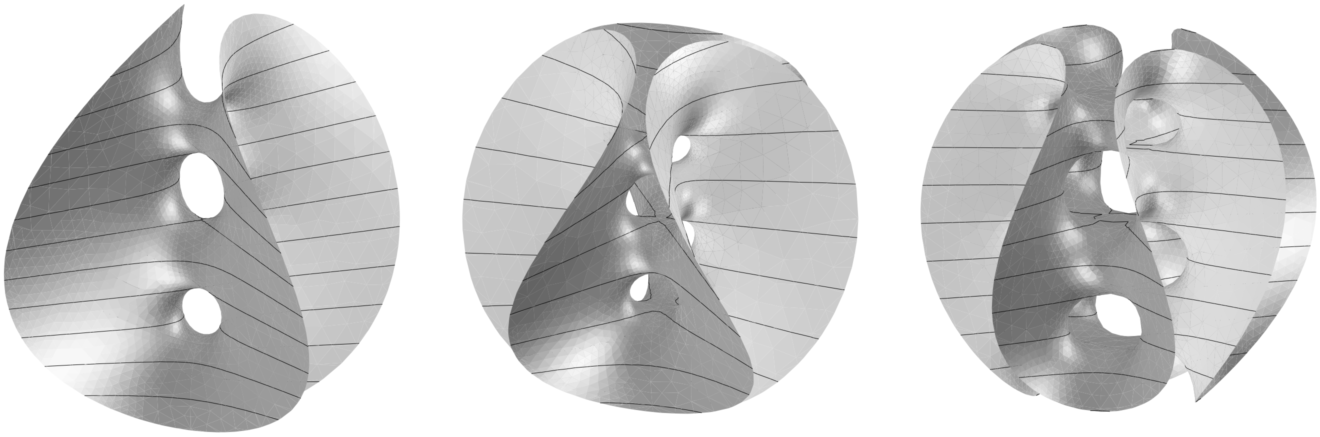

FIGURE 6. Genus-two surface of Chen and Gackstatter (left), and generalizations $M_{2,k}$: in the middle, $k = 3$ (winding order 5), and on the right, $k = 4$ (winding order 7).

With them, the equations in the two-dimensional period problem become

$$\frac{1}{2B}G_1 - \frac{B}{2}F_1 = 0$$

and

$$\frac{1}{2B}\operatorname{Re}(ie^{-i\pi(k-1)/k})G_2 + \frac{B}{2}\operatorname{Re}(ie^{i\pi(k-1)/k})F_2 = 0,$$

which we can rewrite as

$$G_1 = B^2F_1 \quad \text{and} \quad G_2 = B^2F_2$$

or, equivalently,

$$G_1 = B^2F_1, \tag{4.2}$$

$$G_1F_2 = F_1G_2. \tag{4.3}$$

As we observed in the discussion of the general period problem, F_1 and G_1 are nonzero and have the same sign, so (4.2) determines B, for any q_2. Hence we need only find a value of q_2 for which (4.3) is valid.

We will show that $G_1F_2 \le F_1G_2$ for q_2 sufficiently large, and that $G_1F_2 \ge F_1G_2$ for q_2 very near 1. Then, by the intermediate value theorem, a value of $q_2 > 1$ exists such that (4.3) holds.

Applying several changes of variables, we have

$$F_1 = \int_0^1 \sqrt[k]{\left(\frac{(q_2-1+z)(q_2+1-z)}{2-z}\right)^{k-1}} \sqrt[k]{\left(\frac{1-z}{z}\right)^{k-1}}\,dz$$

$$G_1 = \int_0^1 \sqrt[k]{\left(\frac{1+z}{(q_2+z)(q_2-z)}\right)^{k-1}} \sqrt[k]{\left(\frac{1-z}{z}\right)^{k-1}}\,dz$$

$$F_2 = \int_0^{q_2-1} \sqrt[k]{\left(\frac{(1+z)(z+1+q_2)}{2+z}\right)^{k-1}} \sqrt[k]{\left(\frac{q_2-1-z}{z}\right)^{k-1}}\,dz$$

$$G_2 = \int_0^{q_2-1} \sqrt[k]{\left(\frac{q_2-z+1}{(q_2-z)(2q_2-z)}\right)^{k-1}} \sqrt[k]{\left(\frac{q_2-1-z}{z}\right)^{k-1}}\,dz$$

By using the bounds on the values of z over which each term is integrated, we get

$$F_1 \ge \int_0^1 \sqrt[k]{\left(\frac{q_2(q_2-1)}{2}\right)^{k-1}} \sqrt[k]{\left(\frac{1-z}{z}\right)^{k-1}}\,dz,$$

$$G_1 \le \int_0^1 \sqrt[k]{\left(\frac{2}{q_2(q_2-1)}\right)^{k-1}} \sqrt[k]{\left(\frac{1-z}{z}\right)^{k-1}}\,dz,$$

$$F_2 \le \int_0^{q_2-1} \sqrt[k]{\left(2q_2\right)^{k-1}} \sqrt[k]{\left(\frac{q_2-1-z}{z}\right)^{k-1}}\,dz,$$

$$G_2 \ge \int_0^{q_2-1} \sqrt[k]{\left(\frac{1}{2q_2}\right)^{k-1}} \sqrt[k]{\left(\frac{q_2-1-z}{z}\right)^{k-1}}\,dz.$$

Hence

$$F_1G_2 \geq \int_0^1 \sqrt[k]{\Big(\frac{q_2(q_2-1)}{2}\Big)^{k-1}} \sqrt[k]{\Big(\frac{1-z}{z}\Big)^{k-1}}\,dz \times \int_0^{q_2-1} \sqrt[k]{\Big(\frac{1}{2q_2}\Big)^{k-1}} \sqrt[k]{\Big(\frac{q_2-1-z}{z}\Big)^{k-1}}\,dz$$

and

$$G_1F_2 \leq \int_0^1 \sqrt[k]{\Big(\frac{2}{q_2(q_2-1)}\Big)^{k-1}} \sqrt[k]{\Big(\frac{1-z}{z}\Big)^{k-1}}\,dz \times \int_0^{q_2-1} \sqrt[k]{\Big(2q_2\Big)^{k-1}} \sqrt[k]{\Big(\frac{q_2-1-z}{z}\Big)^{k-1}}\,dz.$$

For $q_2 > 1$ sufficiently large we have

$$\sqrt[k]{\Big(\frac{2}{q_2-1}\Big)^{k-1}} \leq \sqrt[k]{\Big(\frac{q_2-1}{2}\Big)^{k-1}}.$$

Hence $G_1F_2 \leq F_1G_2$ for these values.

On the other hand, writing $q_2 = 1+\varepsilon$,

$$\begin{aligned}
F_1 &= \int_0^1 \sqrt[k]{\Big(\frac{(\varepsilon+z)(2+\varepsilon-z)}{2-z}\Big)^{k-1}} \sqrt[k]{\Big(\frac{1-z}{z}\Big)^{k-1}}\,dz \\
&\leq \int_0^1 \sqrt[k]{\Big(\frac{\varepsilon+2}{2}(\varepsilon+z)\Big)^{k-1}} \sqrt[k]{\Big(\frac{1-z}{z}\Big)^{k-1}}\,dz, \\
G_1 &= \int_0^1 \sqrt[k]{\Big(\frac{1+z}{(1+\varepsilon+z)(1+\varepsilon-z)}\Big)^{k-1}} \sqrt[k]{\Big(\frac{1-z}{z}\Big)^{k-1}}\,dz \\
&\geq \int_0^1 \sqrt[k]{\Big(\frac{1}{2+\varepsilon}\,\frac{1}{1+\varepsilon-z}\Big)^{k-1}} \sqrt[k]{\Big(\frac{1-z}{z}\Big)^{k-1}}\,dz, \\
F_2 &= \int_0^\varepsilon \sqrt[k]{\Big(\frac{(1+z)(z+2+\varepsilon)}{2+z}\Big)^{k-1}} \sqrt[k]{\Big(\frac{\varepsilon-z}{z}\Big)^{k-1}}\,dz \\
&\geq \int_0^\varepsilon \sqrt[k]{\Big(\frac{\varepsilon-z}{z}\Big)^{k-1}}\,dz, \\
G_2 &= \int_0^\varepsilon \sqrt[k]{\Big(\frac{2+\varepsilon-z}{(1+\varepsilon-z)(2+2\varepsilon-z)}\Big)^{k-1}} \sqrt[k]{\Big(\frac{\varepsilon-z}{z}\Big)^{k-1}}\,dz \\
&\leq \int_0^\varepsilon \sqrt[k]{\Big(\frac{\varepsilon-z}{z}\Big)^{k-1}}\,dz.
\end{aligned}$$

Therefore

$$F_1G_2 \leq \int_0^1 \sqrt[k]{\big(\tfrac12(\varepsilon+2)(\varepsilon+z)\big)^{k-1}} \sqrt[k]{\Big(\frac{1-z}{z}\Big)^{k-1}}\,dz \times \int_0^\varepsilon \sqrt[k]{\Big(\frac{\varepsilon-z}{z}\Big)^{k-1}}\,dz$$

and

$$G_1F_2 \geq \int_0^1 \sqrt[k]{\Big(\frac{1}{2+\varepsilon}\,\frac{1}{1+\varepsilon-z}\Big)^{k-1}} \sqrt[k]{\Big(\frac{1-z}{z}\Big)^{k-1}}\,dz \times \int_0^\varepsilon \sqrt[k]{\Big(\frac{\varepsilon-z}{z}\Big)^{k-1}}\,dz.$$

For $\varepsilon > 0$ sufficiently small,

$$\sqrt[k]{\Big(\frac{1}{2+\varepsilon}\,\frac{1}{1+\varepsilon-z}\Big)^{k-1}} \geq \sqrt[k]{\Big(\frac{\varepsilon+2}{2}(\varepsilon+z)\Big)^{k-1}}.$$

Hence $G_1F_2 \geq F_1G_2$ for such values of $\varepsilon = q_2 - 1$.

We have shown that there exist values for $B > 0$ and $q_2 > 1$ for which both (4.2) and (4.3) hold; therefore the two-dimensional period problem associated to $M_{2,k}$ can be solved for $k \geq 3$. In other words, $M_{2,k}$ exists:

Theorem 4.1. *For each integer $k \geq 3$, there exists an immersed minimal surface of genus $2(k-1)$ with one generalized Enneper-type end of winding order $2k-1$.*

5. NUMERICAL RESULTS

Researchers in minimal surface theory often have used the computer to search for numerical solutions to the period problem. In this section we describe work on the period problem for the general CGK surfaces $M_{p,k}$ given by (3.3). More precisely, we want to find a zero for the function $\Omega = (\Omega_1, \dots, \Omega_p) : \mathbb{R}^p \to \mathbb{R}^p$ with components

$$\Omega_j(B, q_2, q_3, \dots, q_p) = \begin{cases} \operatorname{Re} \displaystyle\int_{z=q_{j-1}}^{z=q_j} \tfrac12(g^{-1}-g)\,dz & \text{if } j \text{ is odd}, \\ \operatorname{Re} \displaystyle\int_{z=q_{j-1}}^{z=q_j} \tfrac12(g^{-1}+g)\,dz & \text{if } j \text{ is even}, \end{cases} \tag{5.1}$$

where $g = B\, w^{k-1}$,

$$w^k = \begin{cases} zH_p(z, q_1, \dots, q_p) & \text{if } p = 2m, \\ \dfrac{z}{z^2 - q_p^2} H_p(z, q_1, \dots, q_p) & \text{if } p = 2m+1, \end{cases}$$

and

$$H_p(z, q_1, \dots, q_p) = \prod_{l=1}^{m} \frac{z^2 - q_{2l}^2}{z^2 - q_{2l-1}^2}.$$

Recall that we normalized the sphere $M_{p,k}/R_k$ in such a way that $q_1 = 1$. We will refer to the period problem associated with the surface $M_{p,k}$ as $S_{p,k}$.

Historically, the computer has been used to solve one-dimensional period problems, and the elementary bisection method was adequate in these cases. Providing the bisection method with an interval in which a zero is thought to be found, the algorithm evaluates the function at the endpoints, and based on these values it bisects the interval until a zero is approached. But since we intended to consider period problems of arbitrary dimension and zeros can not be bracketed in higher dimensions, we sought an algorithm that would generalize to higher dimensions more easily.

In searching for such an algorithm, we considered several numerical methods designed to find the minimum of a function $\mathcal{S} : \mathbb{R}^p \to \mathbb{R}$. Taking

$$\mathcal{S}(B, q_2, q_3, \dots, q_p) := \sum_{j=1}^{p} \Omega_j^2(B, q_2, q_3, \dots, q_p),$$

we change the problem from one of finding a zero to one of finding a minimum for this new nonnegative function, in the hope that the minimum value is zero. Additionally, since each evaluation of the functions Ω_j involves integral calculations, we sought algorithms that did not require computation of the partial derivatives of $\mathcal{S}$.

The algorithm we chose was the downhill simplex method in multidimensions [Nelder and Mead 1965] (see also [Press et al. 1986, pp. 289–293]). It starts with an initial simplex in $\mathbb{R}^p$, near which one expects to find a zero for $\mathcal{S}$. By comparing the value of $\mathcal{S}$ on the vertices of this simplex, the algorithm moves one or more vertices "downhill" toward lower values of the function, thereby producing a new simplex. Feeding this new simplex back into the algorithm again, one hopes to converge to a local minimum. Most simplex modifications are expected to be "reflections", where the vertex with the highest value is reflected across the opposite face of the simplex. Once the algorithm reaches a valley, it tries to contract itself into the valley and then slide down the valley to lower values for $\mathcal{S}$. Clearly, sharp dimples in the valley floor may cause the algorithm to contract in all directions until it settles at the bottom of the dimple. Figure 7 depicts some possible simplex modifications resulting from one iteration of the method.

To simplify the input of the initial data for this algorithm, we generate our simplices by constructing p other vertices, $x_j = x_0 + \varepsilon e_j$, from a single point $x_0 \in \mathbb{R}^p$, where $(e_1, e_2, \dots, e_p)$ is the standard basis for $\mathbb{R}^p$. The initial simplex is then the one whose vertices are $x_0, x_1, \dots, x_p$.

We tested the algorithm (and our code) by considering the original surfaces $M_{1,2}$ and $M_{2,2}$ proved to exist by Chen and Gackstatter. The numerical solutions found for these surfaces turned out to be correct, so we started searching for solutions to the period problem $S_{3,2}$ associated to $M_{3,2}$, which was not known to exist at the time of the computation. After finding the solution to this three-dimensional period problem, we moved on to the four-dimensional problem for $S_{4,2}$, and ultimately continued this process by searching for solutions to $S_{p+1,2}$ once we had the solutions for $S_{p,2}$. We stopped doing computer searches once we reached $p = 34$. Two of the solutions are illustrated in Figure 8.

It is important to keep in mind that each new period problem $S_{p,2}$ required an initial simplex, or at least an initial point, in $\mathbb{R}^p$, to get the search algorithm started. As p became large, it became more and more difficult to find such initial data; from random initial data, the algorithm tended to converge to degenerate solutions (those where two or more q_j's coincided). If, on the other hand, the initial guess was near enough to a nondegenerate

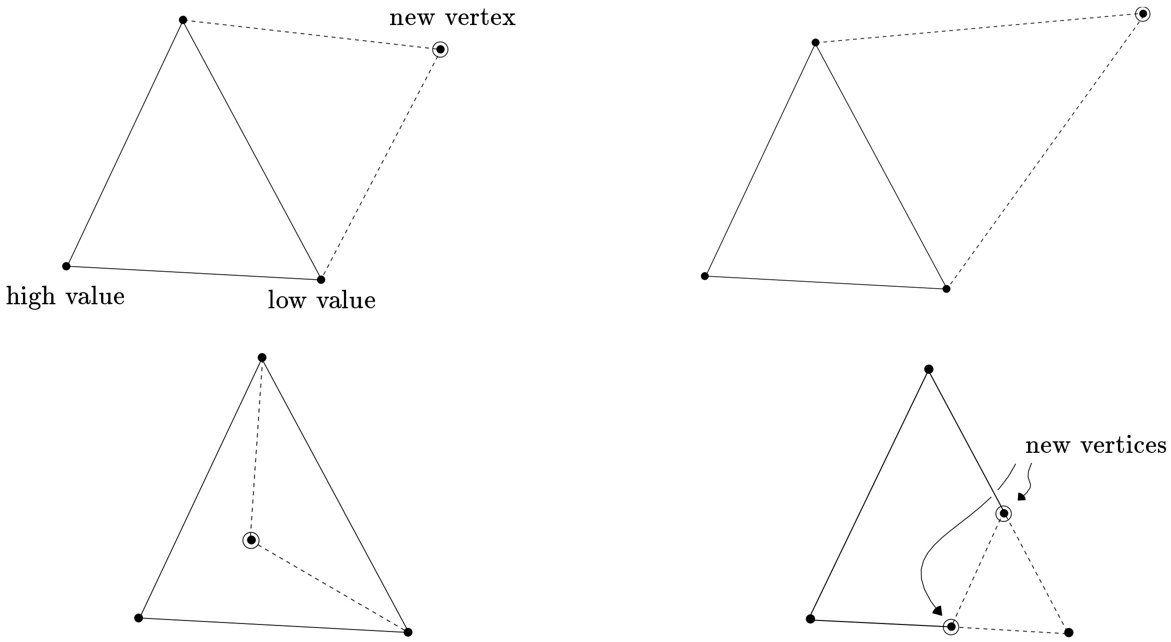

FIGURE 7. Possible modifications of a two-dimensional simplex during one step of the downhill simplex method. The initial simplex is drawn with solid lines while the modified simplex has dashed lines and can be either reflected away from a high point (top left), reflected and expanded (top right), contracted in one dimension away from a high point (bottom left), or contracted along all directions towards a low point (bottom right).

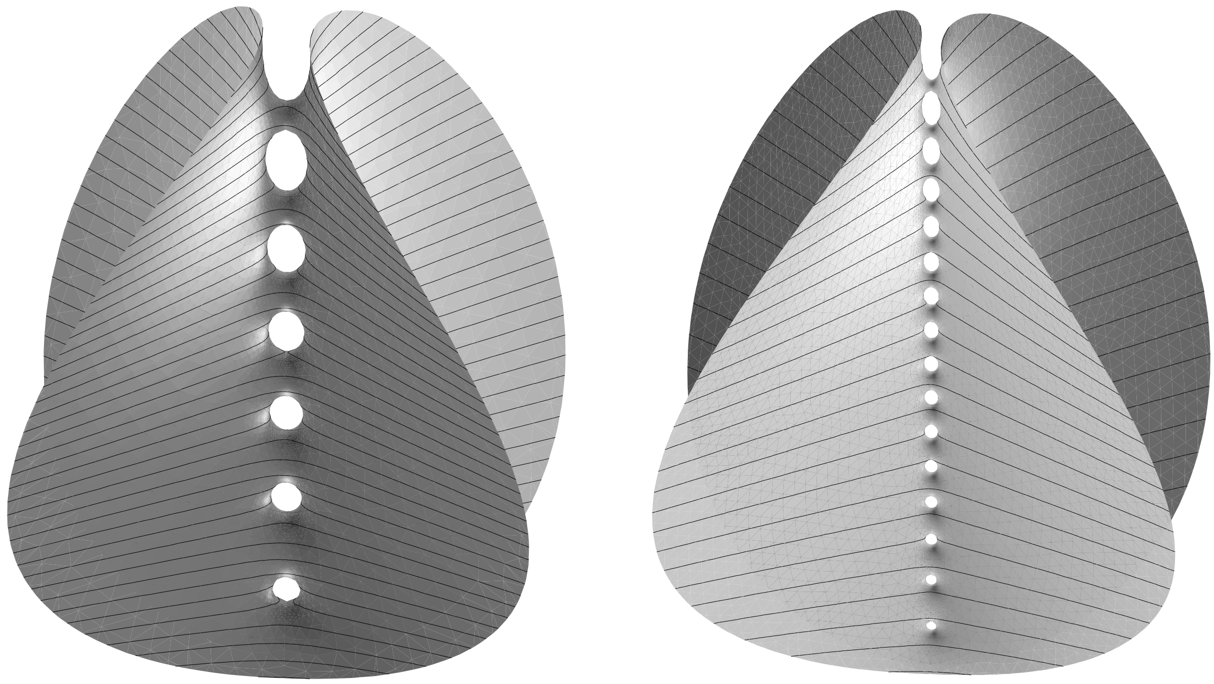

FIGURE 8. Images of $M_{6,2}$ (left) and $M_{15,2}$ (right) made from numerical approximations of the associated six-dimensional and fifteen-dimensional period problems.

solution, the algorithm easily converged to these solutions. At that point we started looking for information that might allow us to predict where in $\mathbb{R}^p$ a solution might be found for $S_{p,2}$. Surprisingly, we found some good predictors.

The most productive idea was to return to the original Weierstrass data and choose another normalization for the coordinate z on $M_{p,2}/R_2$. Instead of choosing z so that $z(Q_1/R_2) = 1$, we choose z so that the branch point for the Gauss map occurs at a specific point along the imaginary axis, which has a net effect of setting B constant at 1. Geometrically, this new normalization corresponds to a homothety of the surface $M_{p,2} \subset \mathbb{R}^3$. Instead of viewing the component period functions Ω_j as functions of $B, q_2, \ldots, q_p$, we now view them as functions of $q_1, q_2, \ldots, q_p$. Using this normalization, we generated the table of solutions to $S_{p,2}$ found in Figure 9 (top), where each horizontal line corresponds to a distinct value of p and the tick marks denote the values of the q_j's solving $S_{p,2}$.

The patterns found in tables of this form for solutions of $S_{p,2}$ for $p < 9$ allowed us to predict where the next solution might be found. Although we have no explaination at this point for the obvious pairing of the values q_j and q_{j+1}, nor for the general "curves" seen in this data, it is our opinion that, without these observations, searches in $\mathbb{R}^p$ for solutions to $S_{p,2}$ with $p > 10$ would mostly yield degenerate solutions.

Soon after making these calculations, we started on the generic problem $S_{p,k}$. To our surprise, the solutions for $S_{p,2}$ were very near nondegenerate solutions for $S_{p,k}$ for k near 2, and for larger k, the nearest known solution generally served as an excellent initiator. Using this observation, we have found solutions to $S_{p,k}$ for $p < 35$ and $k < 10$.

Returning to the original normalization for the coordinate z on the sphere $M_{p,k}/R_k$, and transforming the solutions of $S_{p,k}$ to reflect this other normalization, we produced the data in Figure 9 (bottom). Here the first patterns are less obvious, but another one emerges. Now, it becomes believable that under the normalization $q_1 = 1$, the q_j's nearest zero appear to become evenly distributed, while the larger values demonstrate a stretch/pull phenomenon that is still not understood. In the limit, the end of $M_{p,k}$ appears to be pushed to infinity, and the handles become evenly distributed along the x_3-axis. This suggests the following conjecture.

Conjecture 5.1. *If $M_{p,k}$ exists for all $p > 0$ and $k > 2$, then, for fixed k and $p \to \infty$, with a homothety normalization, the surfaces $M_{p,k}$ converge to the Karcher saddle tower* [Karcher 1988] *with normal rotational symmetry of order k.*

We cannot prove this conjecture. However, assuming it to be true, we were led to the correct Weierstrass data for the saddle towers viewed as complete surface in $\mathbb{R}^3$ of infinite genus, which we explain in Section 6. The critical observations in this process were: first, that the conjecture implied that the values q_j, which solve the period problem $S_{p,k}$, become equidistant along the real axis as p gets large; second, that the algebraic equation for the underlying Riemann surface $M_{p,k}$ then becomes a truncation to the first $2p+1$ terms of the infinite product expansion for $\tan z$. Based on these observations, we started the period calculations for $S_{p,k}$ for $p \geq 400$, with initial data $q_j = j$. In so doing, we observed that the periods nearest the point $\mathcal{O}$ are nearly zero, while those far from this point can be quite large.

6. A GLOBAL REPRESENTATION OF KARCHER'S SADDLE TOWERS

Scherk's original paper [1835] announced the existence of a family of *singly periodic* embedded minimal surfaces. Taking the periodic direction to be vertical, one can think of Scherk's examples as a minimal desingularization of two planes in $\mathbb{R}^3$ meeting along the x_3-axis. See Figure 10 (left).

This heuristic suggested to H. Karcher a generalization of Scherk's surfaces that desingularizes k planes in $\mathbb{R}^3$, all meeting along the x_3-axis, for $k \geq 3$. He succeeded [Karcher 1988] in constructing

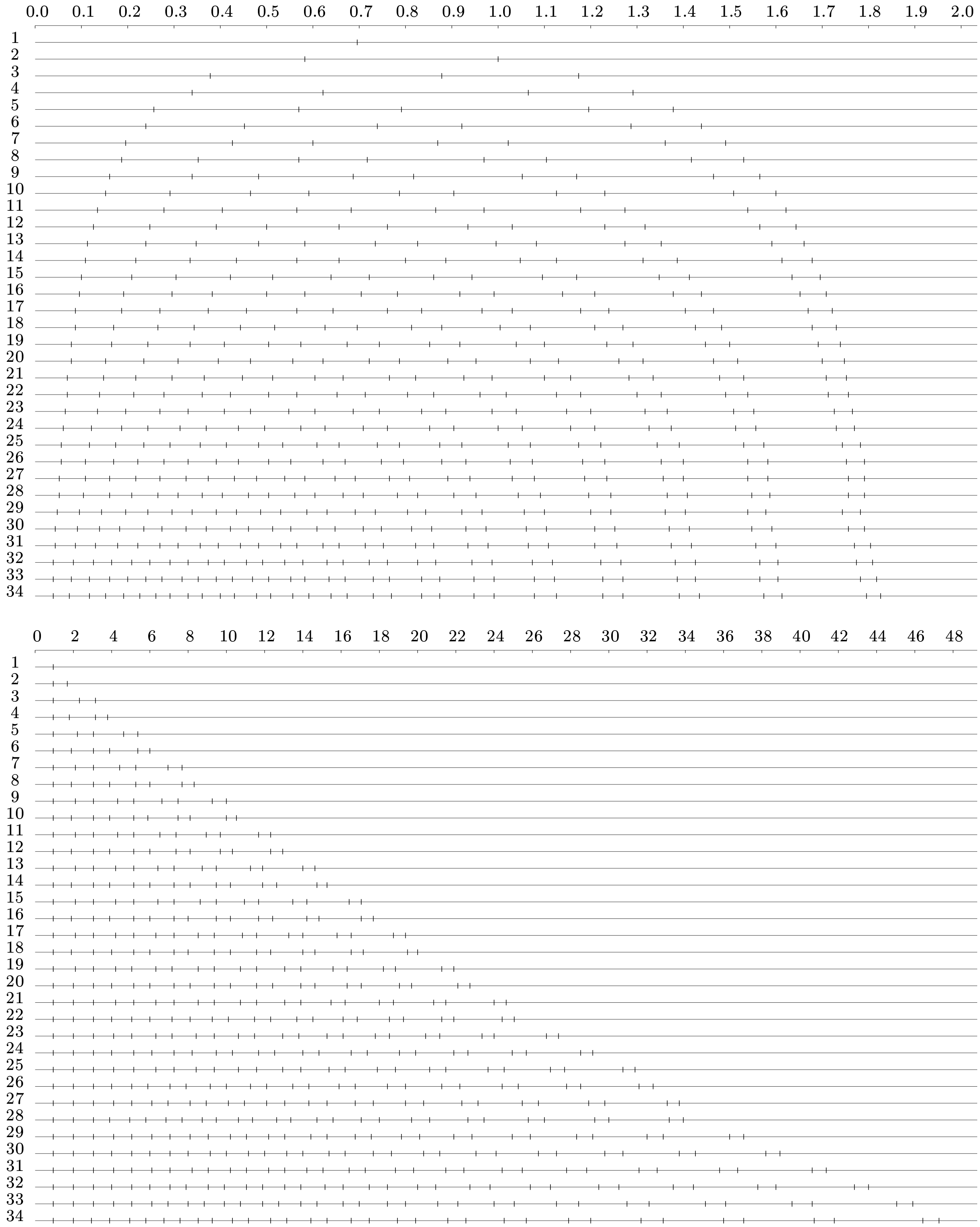

FIGURE 9. Period solutions for $M_{p,2}, p = 1, 2, \ldots, 34$. Top: normalization $B = 1$. Bottom: normalization $q_1 = 1$.

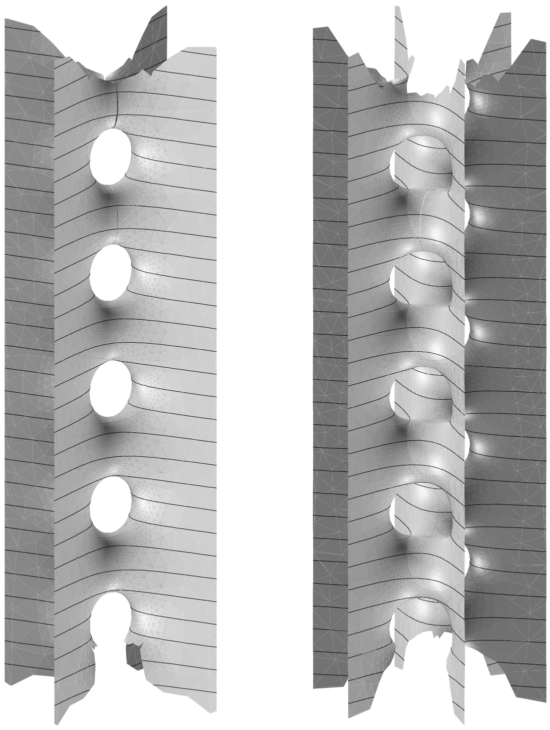

FIGURE 10. Karcher saddle towers drawn from global data for $k = 2$ (left), and 3, (right) with $\alpha = 0$ or $\varphi = \pi/(2k)$.

these surfaces, which he called *saddle towers*, and which we denote here by $S_{k,\varphi}$, for $0 < \varphi \leq \pi/(2k)$. See Figure 10 (right) for an image of $S_{3,\,\pi/(2k)}$.

Two nonparallel planes in $\mathbb{R}^3$ can be completely described, up to Euclidean motion, by the angle between them, which we take as the parameter for Scherk's family. Given k planes, $k \geq 3$, with a common line of intersection, there are more possibilities. The first case considered by Karcher is the maximally symmetric one, where the angle between successive half-planes equals π/k. These saddle towers are called *symmetric*, and we denote them here by $S_{k,\pi/(2k)}$. A *wing* of a saddle tower is the portion of the surface asymptotic to a half plane. Our notation is chosen because these surfaces have $2k$ planar reflectional symmetries, one between each pair of successive wings, and we measure the angle from these planar geodesics. On $S_{k,\pi/(2k)}$, the limit normals to the wings are the horizontal vectors whose stereographic projections equal $i\xi$, where $\xi^{2k} = 1$.

Karcher generalized these examples by constructing the surfaces $S_{k,\varphi}$, for $0 < \varphi < \pi/(2k)$, where this angle is changed so that the limit normals are $e^{\pm i\varphi}\xi$. We refer to the $S_{k,\varphi}$ as *symmetrically deformed* saddle towers. For some values of φ, these surfaces are no longer embedded.

Since $S_{k,\varphi}$ is singly periodic and nonflat, it has infinite total curvature. But, by factoring $\mathbb{R}^3$ by the translational symmetry of $S_{k,\varphi}$, one produces a minimal surface of finite total curvature in $\mathbb{R}^2 \times S^1$. On this surface, Karcher assumed a planar reflectional symmetry corresponding to inversion of the Gauss map through the unit circle. He also assumed that the fundamental domain of this reflection had $2k$ distinct planes of reflectional symmetry that meet along the vertical axis. This axis intersects the surface at the saddle points. The order-preserving symmetries generated by these reflections form a normal rotational symmetry of order k around this axis.

Using these symmetries and the end behavior, Karcher determined the data for $S_{k,\varphi}$ to be

$$\begin{aligned} g &= \xi^{k-1}, \\ \varphi_3 &= \frac{1}{\xi^k + \xi^{-k} - 2\cos(k\varphi)}\,\frac{d\xi}{\xi}, \end{aligned} \tag{6.1}$$

where $0 < \varphi \leq \frac{\pi}{2k}$.

We now prove the following result:

Theorem 6.1. *Let*

$$M_{k,\alpha} = \{(z,w) \in \mathbb{C} \times \mathbb{P}^1 : w^k = \tan z \cos\alpha + \sin\alpha\},$$

where $\alpha \in [0, \pi/2)$. *The mapping* $X : M_{k,\alpha} \to \mathbb{R}^3$ *defined by* (2.1) *with*

$$\begin{aligned} g &= w^{k-1}, \\ \varphi_3 &= dz \end{aligned} \tag{6.2}$$

is a conformal diffeomorphism between $M_{k,\alpha}$ *and* $S_{k,\varphi}$, *where* $\alpha = \pi/2 - k\varphi$.

Remark 6.2. The symmetric saddle towers correspond to $\alpha = 0$, so that $M_{k,0}$ is defined by

$$w^k = \tan z = \prod_{l=1}^{\infty} \frac{z^2 - (2l\pi)^2}{z^2 - ((2l-1)\pi)^2}.$$

Truncation of this infinite product expansion of the tangent function produces the algebraic equations for $M_{p,k}$. The poles and zeros for this truncation must be adjusted so as to solve the period problem on $M_{p,k}$. Truncations of the general infinite product expansions ($\alpha \neq 0$) have been investigated in the hope of finding new minimal surfaces of finite total curvature that may converge to the $S_{k,\varphi}$. In general, this corresponds to removing the restriction that the q_j be strictly real, allowing them to vary over the entire complex numbers. When the period problems associated with these truncations were fed into the same software used for the periods of $M_{p,k}$, the solutions were observed to converge to values associated with the more symmetric examples $M_{p,k}$—that is, the q_j approached real numbers as the periods approached zero.

Proof. In order to make a comparison between the two representations (6.1) and (6.2), we restrict the data in (6.2) to

$$B = \left\{(z,w) \in M_{k,\alpha} : -\frac{\pi}{4} - \frac{\alpha}{2} < \operatorname{Re} z \leq \frac{3\pi}{4} - \frac{\alpha}{2}\right\}.$$

Using basic properties of the tangent function, we see that g on B is a bijective mapping onto $\mathbb{P}^1 \setminus \{w : w^k = ie^{\pm i\alpha}\}$. Comparison of the two Gauss maps suggests the following relationship between ξ and z:

$$\xi = (\tan z \cos\alpha + \sin\alpha)^{1/k}.$$

Performing this change of variable on φ_3 in (6.1), we see that the height differentials differ by a real constant dependent on k and α. Therefore, up to homothety, $X(B)$ is congruent to a fundamental domain of $S_{k,\alpha}$.

We next show that $\partial X(B)$ consists of planar geodesics, from which it follows that $X(M_{k,\alpha})$ and $S_{k,\varphi}$ are congruent. Let $\beta_{j,l} = (\gamma_j(t), w_l(\gamma_j(t)))$, where $\gamma_j(t) = -\pi/4 + j\pi - \alpha/2 + i\,t$, $t \in \mathbb{R}, j = 0, 1$, and w_l, $0 \leq l \leq k-1$, denotes the l-th sheet over γ_j. Noting that

$$\tan z \cos\alpha + \sin\alpha = \frac{\sin(z+\alpha)}{\cos z},$$

we have

$$\begin{aligned} w^k(\gamma_0(t)) &= \frac{\sin\left(-\frac{\pi}{4} + \frac{\alpha}{2} + i\,t\right)}{\cos\left(-\frac{\pi}{4} - \frac{\alpha}{2} + i\,t\right)} \\ &= \frac{\sin\left(-\frac{\pi}{4} + \frac{\alpha}{2}\right)\cosh t + i\cos\left(-\frac{\pi}{4} + \frac{\alpha}{2}\right)\sinh t}{\cos\left(-\frac{\pi}{4} - \frac{\alpha}{2}\right)\cosh t - i\sin\left(-\frac{\pi}{4} - \frac{\alpha}{2}\right)\sinh t} \\ &= \frac{-a\cosh t + ib\sinh t}{a\cosh t + ib\sinh t}, \end{aligned}$$

where

$$\begin{aligned} a &= \cos(-\pi/4 - \alpha/2), \\ b &= \cos(-\pi/4 + \alpha/2). \end{aligned}$$

Hence w^k on $\beta_{0,l}$ is unitary, and therefore so is $g = w^{k-1}$. Therefore $(dg/g)(\beta'_{0,l}) \subset i\mathbb{R}$, so that $\mathrm{II}(\beta_{0,l}) \subset \mathbb{R}$. Since the automorphism of $M_{k,\alpha}$ induced by $z \mapsto -\bar{z} - \pi/2 - \alpha$ is an isometry fixing $\beta_{0,l}$, we see that $\beta_{0,l}$ is a geodesic. By Lemma 2.1 it is planar. A similar analysis for $j = 1$ reveals that $g(\beta_{1,l})$ is unitary and $\beta_{1,l}$ is a geodesic.

We have shown that $\partial X(B)$ consists of $2k$ planar geodesics. Extending $X(B)$ across these curves by Schwarz reflection produces a surface that agrees with $X(M_{k,\alpha})$, so $X(M_{k,\alpha})$ is congruent to $S_{k,\varphi}$. This completes the proof. □

6.1. A Global Representation of Scherk's Doubly Periodic Surfaces

Scherk's 1835 paper also describes a one parameter family of embedded doubly periodic minimal surfaces in $\mathbb{R}^3$. Factoring any surface in the family by its two translational symmetries produces a minimal sphere in $T \times \mathbb{R}$ with four points removed, where T is a rhombic torus and the puncture points represent the ends. With the traditional orientation and position of this surface in $\mathbb{R}^3$, the stereographic projection of the limit-normals

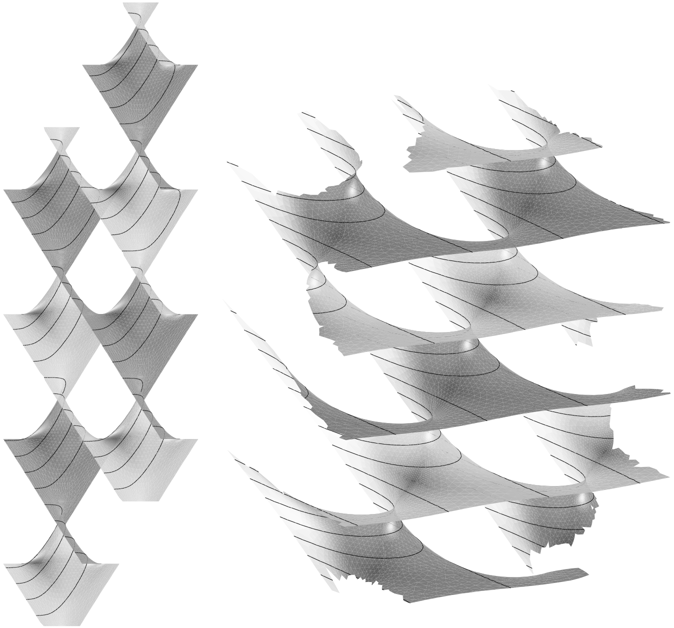

FIGURE 11. Two views of Scherk's deformation of S_0. The image on the left is computed in the quotient and the one on the right is computed by global data.

at these ends is $\pm e^{\pm i\theta}$, for $\theta \in (0, \pi/4]$. Consecutive 90° rotations about the x_2 and x_3 axes reposition the surface so that the values omitted by the stereographic projection of the Gauss map become $\{0, \infty, \alpha i, -\alpha^{-1} i\}$, with $\alpha \in (0, 1]$. We choose to use α as the deformation parameter, and denote the complete surface in $\mathbb{R}^3$ by S_α, and its quotient in $T \times \mathbb{R}$ by $\tilde{S}_\alpha$. In this section we describe the global representation of the surfaces S_α, but first we review its quotient representation.

Since the quotient surface is conformally a sphere with four ends and the Gauss map is injective, we parametrize it by this map. The end behavior, together with the fact that the height differential has no zeros at finite points, determines the height differential up to a nonzero multiplicative complex constant. The absolute value of this factor is chosen to simplify a later calculation and corresponds to a rescaling in $\mathbb{R}^3$. The phase of the multiplicative constant is determined to be zero by the behavior of the data along the straight lines on the surface. Therefore, the Weierstrass data for $\tilde{S}_\alpha$ in $T \times \mathbb{R}$ is

$$g = \xi,$$
$$\varphi_3 = \frac{\alpha^2 + 1}{2} \frac{d\xi}{(\xi - \alpha i)(\xi + \alpha^{-1} i)},$$

where ξ is the standard coordinate on $\mathbb{C} \setminus \{0, \alpha i, -\alpha^{-1} i\}$. The Weierstrass representation given by this data is multivalued with two linearly independent periods.

Using arguments similar to those used for the saddle towers, we can prove the following result:

Theorem 6.3. *S_α is conformally diffeomorphic to*

$$M_\alpha := \left\{ (z, w) \in \mathbb{C}^2 : e^w = -i \frac{e^{iz} - \alpha e^{-iz}}{\alpha e^{iz} + e^{-iz}} \right\}$$

via the mapping $X : M_\alpha \to \mathbb{R}^3$ defined by (2.1), *with*

$$g = e^w$$
$$\varphi_3 = dz.$$

When $\alpha = 1$, this data simplifies to $e^w = \tan z$, which corresponds to the most symmetric Scherk surface.

Remark 6.4. With the global representation in this theorem, one sees directly that, as $\alpha \to 0$, the Weierstrass data converges to

$$M_0 := \{(z, w) \in \mathbb{C}^2 : e^w = -ie^{2iz}\} = \mathbb{P}^1,$$
$$g = -ie^{2iz},$$
$$\varphi_3 = dz,$$

which is the global data for the helicoid [Hoffman et al. 1993; Hoffman and Wohlgemuth].

Osserman [1985] made the following observation:

Proposition 6.5. *S_α has infinite genus and one topological end.*

Applying the results of M. Heins, we have an alternative proof of this. Let $f : \mathbb{C} \to \mathbb{C}$ be an analytic function whose zeros are simple and discrete. Heins

[1952] observed that if such a function has at least two zeros, the Riemann surface defined by

$$e^w = f(z)$$

has infinite genus and one end.

Examination of Heins's argument reveals that the same proof applies to the case in which f has discrete simple poles. Hence, together with Theorem 6.3 we have Osserman's result. Given the conformal diffeomorphism presented above, one may follow Osserman's and Heins's arguments in parallel, to see that they are virtually identical.

ACKNOWLEDGEMENTS

We wish to thank Jim Hoffman at the Center for Geometry, Analysis, Numerics, and Graphics, for his help in preparing images.

REFERENCES

[Bloß 1989] D. Bloß, "Elliptische Funktionen und vollständige Minimalflächen", Ph.D. thesis, Freie Universität Berlin, 1989.

[Chen and Gackstatter 1982] C. C. Chen and F. Gackstatter, "Elliptische und hyperelliptische Funktionen und vollständige Minimalflächen vom Ennepershen Typ", *Math. Ann.* **259** (1982), 359–369.

[Callahan et al. 1990] M. Callahan, D. Hoffman, and W. H. Meeks III, "The structure of singly-periodic minimal surfaces", *Inventiones Math.* **99** (1990), 455–481.

[Espírito Santo 1993] N. do Espírito Santo, "Superfícies mínimas completas em $\mathbb{R}^3$ com fim de tipo Enneper", Ph.D. thesis, Instituto de Matemática Pura e Aplicada, Rio de Janeiro, 1993.

[Gackstatter 1976] F. Gackstatter, "Über die Dimension einer Minimalfläche und zur Ungleichung von St. Cohn-Vossen", *Arch. Rational Mech. Anal.* **61**(2) (1976), 141–152.

[Heins 1952] M. Heins, "Riemann surfaces of infinite genus", *Annals of Math.*, **55** (1952), 296–317.

[Hoffman et al. 1993] D. Hoffman, H. Karcher, and F. Wei, "The genus one helicoid and the minimal surfaces that led to its discovery", pp. 119–170 in *Global Analysis and Modern Mathematics* (edited by K. Uhlenbeck), Publish or Perish, Berkeley, 1993.

[Hoffman and Meeks 1985] D. Hoffman and W. H. Meeks III, "A complete embedded minimal surface in $\mathbb{R}^3$ with genus one and three ends", *J. Diff. Geom.* **21** (1985), 109–127.

[Hoffman and Meeks 1988] D. Hoffman and W. H. Meeks III, "A variational approach to the existence of complete embedded minimal surfaces", *Duke J. Math.* **57** (1988), 877–894.

[Hoffman and Meeks 1989] D. Hoffman and W. H. Meeks III, "The asymptotic behavior of properly embedded minimal surfaces of finite topology", *J. Amer. Math. Soc.* **2** (1989), 667–681.

[Hoffman and Meeks 1990] D. Hoffman and W. H. Meeks III, "Embedded minimal surfaces of finite topology", *Annals of Math.* **131** (1990), 1–34.

[Hoffman 1982] D. Hoffman, review of [Chen and Gackstatter 1982], *Math. Reviews*, 1982. Review number 84d:53005.

[Hoffman and Wohlgemuth] D. Hoffman and M. Wohlgemuth, "Limiting behavior of classical periodic minimal surfaces", in preparation.

[Jorge and Meeks 1983] L. Jorge and W. H. Meeks III, "The topology of complete minimal surfaces of finite total Gaussian curvature", *Topology* **22** (1983), 203–221.

[Karcher 1988] H. Karcher, "Embedded minimal surfaces derived from Scherk's examples", *Manuscripta Math.* **62** (1988), 83–114.

[Karcher 1989] H. Karcher, "Construction of minimal surfaces", pp. 1–96 in *Surveys in Geometry*, University of Tokyo, 1989, and Lecture Notes **12**, SFB256, Bonn, 1989.

[Kusner 1987] R. Kusner, "Conformal geometry and complete minimal surfaces", *Bull. Amer. Math. Soc.* **17** (1987), 291–295.

[Lopez 1992] F. J. Lopez. "The classification of complete minimal surfaces with total curvature greater than -12π", *Trans. Amer. Math. Soc.* **334** (1992), 49–74.

[Meeks and Rosenberg 1990] W. H. Meeks III and H. Rosenberg, "The maximum principle at infinity for minimal surfaces in flat three-manifolds", *Comment. Math. Helv.* **65** (1990), 255–270.

[Meeks and Rosenberg 1993] W. H. Meeks III and H. Rosenberg, "The geometry of periodic minimal surfaces", *Comment. Math. Helv.* **68** (1993), 538–578.

[Nelder and Mead 1965] J. A. Nelder and R. Mead, "A simplex method for function minimization", *Computer J.* **7** (1965), 308–313.

[Osserman 1965] R. Osserman, "Global properties of classical minimal surfaces", *Duke J. of Math.* **32** (1965), 565–573.

[Osserman 1986] R. Osserman, *A Survey of Minimal Surfaces* (2nd ed.), Dover, New York, 1986.

[Press et al. 1986] W. Press, B. Flannery, S. Teukolsky, and W. Vetterling, *Numerical Recipes*, Cambridge University Press, Cambridge, 1986.

[Scherk 1835] H. F. Scherk, "Bemerkungen über die kleinste Fläche Innerhalb gegebener Grenzen", *J. reine angew. Math.* **13** (1835), 185–208.

[Schoen 1983] R. Schoen, "Uniqueness, symmetry, and embeddedness of minimal surfaces", *J. Diff. Geom.* **18** (1983), 791–809.

[Traizet] M. Traizet, "New triply periodic minimal surfaces", preprint III.22, GANG, University of Massachusetts, Amherst.

[Wohlgemuth 1993] M. Wohlgemuth, "Vollständige Minimalflächen höheren Geschlechts und endlicher Totalkrümmung", Ph.D. thesis, University of Bonn, 1993.

Software Availability

The code for solving the period problem is available in the form of a C++ function that returns the values of $q_1, q_2, \ldots, q_p$ given $p \leq 34$ and some values of k. Send requests to the author at ed@gang.umass.edu.

The program MESH, created by Jim Hoffman, was used to generate all the surfaces shown. MESH is available by anonymous ftp from ftp.gang.umass.edu, in directory pub/mesh. Questions concerning this distribution should be directed to Dave Oliver at mesh_help@gang.umass.edu.

Edward C. Thayer, Department of Mathematics, University of Massachusetts, 1535 Lederle Graduate Research Center Towers, Amherst, MA 01003

Received November 7, 1994; accepted in revised form March 21, 1995